REVIEWS

Development of novel multiple quantum methodologies for the analyses of complex proton NMR spectra of scalar coupled spins

G. N. Manjunatha Reddy[1] *AND N. Suryaprakash*[2]

Abstract | One of the significant advancements in Nuclear Magnetic Resonance spectroscopy (NMR) in combating the problem of spectral complexity for deriving the structure and conformational information is the incorporation of additional dimension and to spread the information content in a two dimensional space. This approach together with the manipulation of the dynamics of nuclear spins permitted the designing of appropriate pulse sequences leading to the evolution of diverse multidimensional NMR experiments. The desired spectral information can now be extracted in a simplified and an orchestrated manner. The indirect detection of multiple quantum (MQ) NMR frequencies is a step in this direction. The MQ technique has been extensively used in the study of molecules aligned in liquid crystalline media to reduce spectral complexity and to determine molecular geometries. Unlike in dipolar coupled systems, the size of the network of scalar coupled spins is not big in isotropic solutions and the MQ ^{1}H detection is not routinely employed, although there are specific examples of spin topology filtering. In this brief review, we discuss our recent studies on the development and application of multiple quantum correlation and resolved techniques for the analyses of proton NMR spectra of scalar coupled spins.

[1]*Université Paul Cézanne (Aix-Marseille III) Institut des Sciences Moléculaires de Marseille ISM2-UMR-CNRS-6263, Campus Saint Jérôme, Faculté des Sciences et Techniques, Service 512 13397 Marseille cedex 20, France*
[2]*NMR Research Centre, Indian Institute of Science, Bangalore 12, India*
nsp@sif.iisc.ernet.in

1. Introduction

NMR Spectroscopy has proven to be an indispensable tool for the elucidation of molecular structure and conformation both in chemistry and biology. The usefulness of the technique stemmed from the significant shift in the resonance positions of various nuclei, that even microscopic variation in the electronic charge distribution around the nucleus can be detected. The number of observed spectral transitions depends on the various possible interactions experienced by the nuclear spins. Thus with the increased size of the molecules there is a stringent requirement on the spectral resolution implying that the extraction of spectral information from very complex NMR spectra is always a challenging task. One of the significant advancements of NMR spectroscopy in combating this problem is the incorporation of another dimension and to achieve spectral dispersion in a two-dimensional space. This approach combined with the understanding of the dynamics of nuclear spins under the application

of designed sequence of pulses led to the evolution of diverse multidimensional NMR methodologies to extract the desired spectral information in a simplified manner. One such technique is the detection of higher quantum (multiple quantum) NMR frequencies which are generally forbidden according to selection rules of NMR transitions. The detected single quantum NMR transitions are highly redundant and all the transitions are not required to derive interaction parameters. The higher quantum transitions on the other hand reduce this redundancy and simplify the analyses of complex NMR spectra. This method has found excellent applications in the study of structure of molecules aligned in liquid crystalline media. In the isotropic solutions the network of scalar coupled spins are not bigger and multiple quantum (MQ) technique is not generally employed for analyses of the spectra. Nevertheless the concept of MQ is employed in several multi-dimensional experiments such as INADEQUATE, where the correlation between coupled natural abundant ^{13}C spins is detected. Though there are reported studies on spin topology filtering, it is not routinely employed for the analyses of spectra of scalar coupled spins. In this brief review, we discuss our recent studies utilizing spin selective and non-selective multiple quantum correlation and resolved techniques for the simplification of the analyses of complex proton NMR spectra of scalar coupled spins. For more detailed conceptual understanding and the applications of multiple quantum NMR techniques readers are referred to excellent reviews[1,2].

2. The analyses of the isotropic spectra

In the conventional high resolution single quantum (SQ) NMR spectra of diamagnetic materials in liquid or solution states the line positions and the line intensities depend on chemical shifts (δ_i) and the scalar couplings (J_{ij}). The information on the molecular structure and conformation is generally obtained using these parameters. The three bond J_{ij}'s are particularly employed for obtaining the dihedral angle restraints[3–5]. The number of spectral parameters required to be derived depends on the chemical or magnetic equivalence of the spins in the molecules. For N coupled spins, theoretically there are $^{2N}C_{N-1}$ possible transitions from which N chemical shifts and $N*(N-1)/2$ spin-spin couplings are to be determined. The spectral analysis to obtain these parameters could be either first order or second order depending on whether the spin system is strongly or weakly coupled, where the definition of strong and weak coupling is determined by the ratio of the spin-spin coupling to that of the chemical shift difference between the interacting spins. In a weakly coupled spin system, where the chemical shift separation between the interacting spins is several orders of magnitude larger than the spin-spin couplings, the first order analyses of the spectra is generally feasible. Several methodologies have been developed for the analyses of the spectra and the measurement of scalar couplings in weakly coupled spin systems, viz., J-resolved[6–8], E-COSY type[9–16] and quantitative J correlation experiments[17–19]. As far as the determination of the relative signs of the coupling constants is concerned several strategies have been developed over the years, viz., the two dimensional correlation experiments that provide reduced multiplicities like z-COSY[20], Soft-COSY[21] and E-COSY[14]. There are also one dimensional techniques practiced from the early days of NMR to derive such information by spin tickling[22], double and triple resonance[23] experiments.

3. Spin state selective detection

Another methodology which is widely practiced is the spin state selective detection, where the high field and low field components of both resolved and unresolved multiplets are either separated or individually detected, for the measurement of scalar couplings in biological macromolecules and also in high resolution NMR studies in the solid state. The phase sensitive and spin state selective double quantum (DQ) and zero quantum (ZQ) coherence[24–26] studies, where the couplings evolve as sums and differences respectively, provide the magnitudes and signs of scalar couplings. The information on the development of pulse sequences, for spin state selective detection and their implementation in many one and multidimensional experiments, is available in the literature. These include suppression of differential relaxation effects[27], measurement of heteronuclear one-bond coupling constants[28], for accurate measurement of small spin-spin couplings in biological macromolecules dissolved in liquid crystalline phase, wherein the compensated spin-state filter called DIPSAP (Double In Phase Single Anti Phase)[29] is introduced for J-mismatch, in triple resonance experiments to determine three-bond scalar couplings between ^{13}C$^/$ and ^{1}H$^\alpha$ in proteins[30], to remove contributions of the J-coupling to the line width in solid-state NMR[31], resolution enhancement in Multidimensional Solid-State NMR Spectroscopy of Proteins Using Spin-State Selection,[32] efficient strategy has been introduced using In Phase Anti Phase (IPAP) to achieve spin-state-selective editing for all multiplicities in the detection dimension of the HSQC experiment[33], for enhanced resolution in

the ^{13}C solid-state INADEQUATE spectra through Spin-State-Selection by removing J-couplings in both the dimensions of the 2D experiment[34], to distinguish the intra and interresidue connectivities without using the HN(CO)CA experiment[35], to mimic the selective decoupling[36], for measuring the heteronuclear one-bond and homonuclear two-bond couplings from an HSQC-type spectrum[37], COCAINE experiment for the detection of C$^{/}$, C$^{\alpha}$ correlations in proteins using a new time and sensitivity optimal experiment.[38], for the accurate measurement of scalar and residual dipolar couplings using Spin-State-Selection and editing in three dimensions[39], for accurate monitoring of chemical shift in multidimensional NMR[40], for simultaneous spin-state selection for ^{13}C and ^{15}N from a time-shared HSQC-IPAP experiment[41], for increased confidence in cross-correlation rates measurements[42]. Application of spin state selection is most easily employed when the coupling partner has only a single spin with a sizeable J coupling[34]. Thus most of the spin state selective studies are restricted for the weakly coupled spin systems, excitation of double / zero quantum coherence for the heteronuclear correlation and for the extraction of homo- and heteronuclear J couplings between two coupled pairs of spins.

4. Multiple quantum NMR

In spin systems having detectable couplings among the entire coupled spin network, the spectral complexity increases with the increase in the number of interacting spins and with the decrease in the spin symmetry of the molecules. As an example, for a molecule with seven interacting spins and without any spin symmetry there are 3003 theoretically allowed transitions, from which seven chemical shifts and twenty one scalar couplings are to be derived. Thus number of single quantum transitions detected is highly redundant. One of the ways of simplifying the analyses of the spectra is to detect single quantum transitions that are sufficient for extraction of the spectral information. This is achieved by detecting the higher quantum transitions. The direct detection of the higher quantum transitions are forbidden and have to be detected indirectly. This subject documented in the NMR literature as multiple quantum (MQ) NMR resulted in numerous applications[1,2]. A brief description of the principle of MQ is given below.

MQ coherence is a coherent superposition of states for which the total spin quantum number is anything other than ± 1. The spins which undergo flipping between any two energy states are said to be active in the coherence and all the remaining spins are said to be passive. The detected coherence depends both on the order of the quantum and on the properties of active spins and their interactions with the passive spins. The group of active spins can be considered as the super spin and the remaining passive spins as spectator spins. As the size of the super spin increases, the number of spectator spins, consequently the scalar fields experienced by the active spins decreases. Therefore the multiplet pattern of higher quantum coherence will become simpler. The number of allowed transitions for the zeroth and higher order quantum coherence of N interacting spins is given by
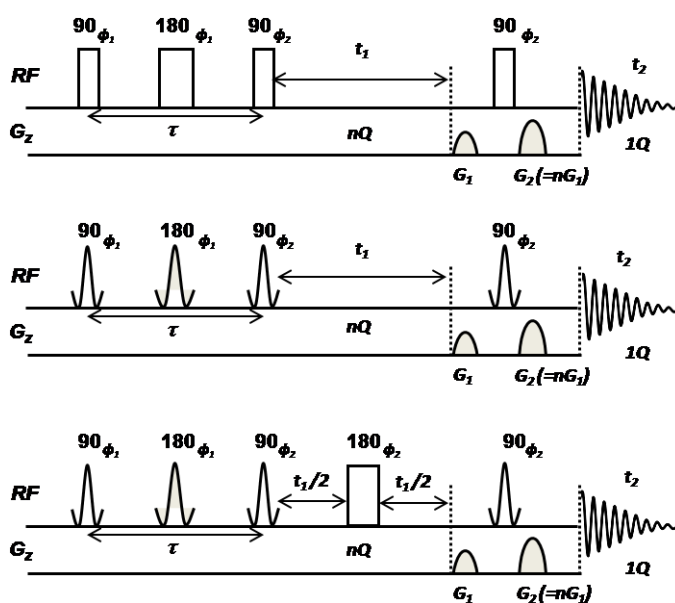
$$Z_0 = 1/2[^{2N}C_N - 2^N] \tag{1}$$

$$Z_m = 2N!/(N-m)!(N+m)! \tag{2}$$

where Z_0 refers to ZQ and Z_m refers to mth quanta for $m \neq 0$. Thus for the N non-equivalent spin $1/2$ system, $N = m$ gives the highest quantum and it pertains to a situation wherein all the spins are participating spins and there are no spectator spins. This corresponds to a situation where all the N spins flips simultaneously from the state $|\alpha\rangle$ to the state $|\beta\rangle$ or vice versa. This implies that the scalar fields do not influence the spectrum. Thus the Nth quantum spectrum of N coupled spins will be at the additive value of their chemical shifts.

$N-1$ quantum is a situation in which $N-1$ spins flip in the presence of one left over spin. The super spin is then split by the scalar field of the spectator spin providing a doublet centered at the sum of the chemical shift positions of the active spins whose separation provides the sum of the couplings of the active spins to the passive spin. N non-equivalent spins thus provides N doublets in the $N-1$ quantum. The $N-2$ quantum spectrum is a situation where $N-2$ spins flip at a time in the presence of remaining spins. This will have more number of transitions than $N-1$ quantum, but significantly less compared to SQ transitions. Thus the number of transitions and thereby the complexity of the spectrum increases by going to lower quantum. The $N-1$ and $N-2$ quantum spectra have sufficient number of transitions to provide all the spectral parameters[2]. Furthermore, the sensitivity of the precessional frequency of any higher quantum coherence is proportional to its order. Thus the magnetic field inhomogeneity broadens the mth quantum order by m times. However, the zero quantum coherence is insensitive to the field inhomogeneity.

In isotropic solutions the concept of MQ is utilized in experiments such as multiple quantum filtered correlation spectroscopy (MQF-COSY). Another category of experiments belongs to the detection of multiple quantum-single quantum

Figure 1: (A) The pulse sequence used for the non selective MQ-SQ correlation experiments. The delay, τ, to be optimized for the excitation of proton homonuclear MQ, The phases are $\Phi_1 = (p)x$, $\Phi_2 = \Phi_1 = X$ for even quanta and $\Phi_R = Y$ for odd quanta (receiver phase) $= x$, where p is the order of coherence. (B) The pulse sequence used for the spin selective MQ-SQ correlation experiments. All the pulses are selectively applied on super spin. (C) Pulse sequence used for MQ-J resolved experiments, which is identical to B, but the 180° pulse in the middle of t_1 period is non-selective.

(MQ-SQ) correlation. The MQ-SQ experiments can be broadly classified as homonuclear and hetero nuclear type based on the types of nuclei involved in the coherence transfer. The term coherence is used to indicate the precession of nuclear spins in a 3D basis set of spin operators; I_x, I_y and I_z along x, y and z axes. Thus the existence of non-vanishing couplings among the spins is a requirement for coherence transfer to occur. Therefore in the molecules such as benzene and pyrazine where the scalar couplings among the protons are not reflected in the spectrum, it is not possible to detect any higher quantum transitions. In order to represent the MQ coherences the two spin operators like $2I_xS_x$, $2I_xS_y$, $2I_yS_x$ and $2I_yS_y$ and their linear combinations are essential.

5. Multiple quantum using spin-selective and non-selective pulses

The MQ experiments generally employ a three pulse sequence. The multiple quantum orders are created during the evolution period and are later converted into detectable transverse magnetization. Depending on the information to be derived the appropriate excitation and detection pulse sequences are constructed. The pulse sequences generally employed in selective and non-selective MQ

experiments are given in Fig. 1. The information on the MQ spectrum and the derivable information for different types of spin systems are available in the literature[43]. Excitation and detection sequences can be designed from either selective or non-selective pulses. As an example in a homonuclear three spin system of the type AMX, one can non selectively excite all the three possible double quantum transitions, viz. AM double quantum (where A and M spins are active spins), AX double quantum where A and X spins are active spins), and MX double quantum where M and X spins are active spins). In the MQ-SQ correlation experiment the MQ dimension provides three sets of doublets at the sum of the chemical shifts of the two active spins. The separation of the doublets pertains to sum of the passive couplings, viz., J_{AX+MX}, J_{AM+MX} and J_{AM+AX} respectively for AM, AX and MX double quantum. Each component of these doublets corresponds to the $|\alpha\rangle$ and $|\beta\rangle$ states of the passive spin. The cross sections taken along the SQ dimension for any of the spin states of the passive spin, gives all the twelve transitions expected for an AMX spin system, whose intensities depend on the flip angle. Thus in a non selective detection each $|\alpha\rangle$ and $|\beta\rangle$ state of passive spins correlate to all the

allowed transitions in the SQ dimension. The flip angle dependence of the intensities for an AMX spin system has been reported[44].

If a pulse is applied selectively on any two spins and no pulse is applied on the third spin, then the states of the passive spin remain unperturbed both in MQ and SQ dimensions. It may be emphasised that in the selective excitation the spins must be weakly coupled and selective excitation is not possible in strongly coupled spin systems. Due to large chemical shift difference, the heteronuclear spins are weakly coupled. The non-selective excitation of homonuclear highest quantum coherence in heteronuclear spin systems retains the spin states of heteronucleus undisturbed. This is analogous to the selective excitation in a homonuclear spin system and in both the situations the states of the passive spin(s) are unperturbed. This is termed spin state selection and each spin state of the passive spins in the MQ dimension encodes the spin states involved in the SQ transitions that arise only due to coupling among active spins and results in the selective detection of SQ transitions. The cross section taken along SQ dimension for any one of the passive spin states has less number of transitions compared to the normal single quantum spectrum but are suffice to determine the chemical shifts of active spins and the couplings among them. For example in the selective AM double quantum excitation of AMX spin system, the cross section taken along SQ dimension for each spin state of passive X spin provides only four transitions instead of eight. Thus the spin state selection has a power of reducing the spectral complexity. The interesting feature of the experiment is that it also achieves, in homonuclear spin systems, separation of passive couplings and active couplings in the MQ and SQ dimensions respectively. In the heteronuclear spin systems it achieves separation of homo and heteronuclear couplings respectively in direct and indirect dimensions.

The selection of particular higher quantum is achieved by the application of pulsed field gradients before and after the last pulse (G_1 and G_2 in Fig. 1), which converts MQ coherence to detectable SQ coherence. The gradient ratio "n" (G_2/G_1) defines the order of the quantum to be detected. This also implies that zero quantum selection is impossible by the application of gradients. The detection of zero quantum coherence is achieved by phase cycling. In the following sections the application of the spin selective MQ experiments for spectral simplification, such as spin system filtering and the utilization of higher quantum J-resolved techniques for the determination of scalar couplings of smaller magnitudes are discussed taking specific examples.

6. Spin system filtering

As discussed before the SQ transitions are highly redundant. Further the spectra could also be complex due to numerous scalar couplings experienced by each interacting spin. The closely resonating protons present in the same molecule under different chemical environments result in degenerate or near degenerate transitions. Discerning of these degenerate transitions is a prerequisite for spectral analyses. One of the ways of simplifying the analyses is the filtering of spin-coupled networks of different topologies using multiple quantum single quantum correlation[45,46]. These pulse schemes can distinguish molecular fragments containing same number of spins but different coupling topologies. But the creation of multiple quantum coherence is inhibited when the system departs from the specified spin topology. In bigger molecules containing different spin systems, it is possible for their separation by employing non-selective excitation of highest quantum, provided the cumulative additive values of the chemical shifts of active spins are substantially different among different spin systems. Further the spectrum of each such spin system itself may be complex due to the presence of several scalar couplings of diverse magnitudes. Additional spectral simplification can be achieved by the blend of the spin system filtering with spin-state selection. This concept is briefly discussed for homo and heteronuclear spins.
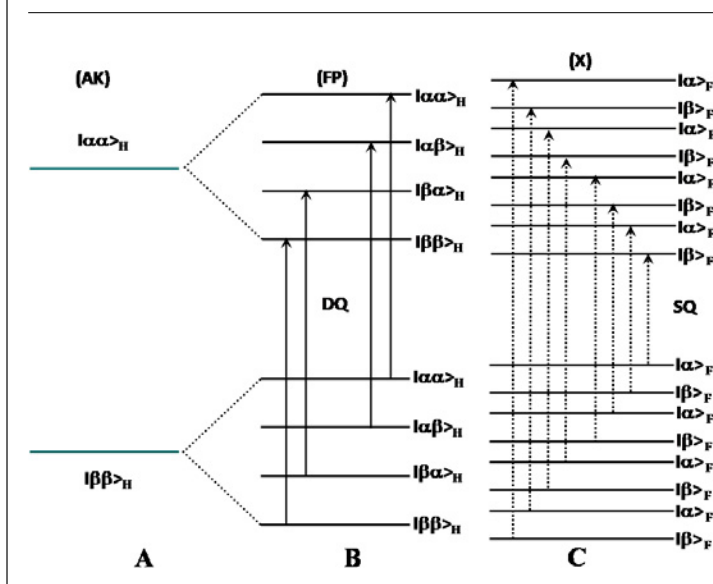
7. Spectral simplification using MQ spin state selection

In homonuclear case, the spin state selection is achieved by the pulse sequence depicted in Fig. 1B. As an example the selective excitation of proton double quantum (DQ) (spins A and K) in a five spin system of the type AFKPX (where $X = {}^{19}$F and the remaining spins are protons), is discussed. Proton is detected in both F_1 and F_2 dimensions and ^{19}F is decoupled in F_1 dimension.

The selective double quantum excitation of A and K spins results in two energy states corresponding to their $|\alpha\alpha\rangle$ and $|\beta\beta\rangle$ spin states. This is depicted in Fig. 2A. In the DQ dimension each of these states are further split into four energy states corresponding to four possible spin states $\alpha\alpha$, $|\alpha\beta\rangle$, $|\beta\alpha\rangle$ and $|\beta\beta\rangle$ of F and P spins giving rise to only four transitions. This is depicted in Fig. 2B. Since ^{19}F is decoupled in F_1 dimension, there is no additional splitting. In the F_2 dimension, normal one dimensional spectrum (SQ) including coupling with ^{19}F spin is detected.

The spin state selection for a heteronuclear spin system AFKPX (where $X = {}^{19}$F and the remaining spins are protons) is pictorially represented by an

Figure 2: The schematic representation of energy level diagram depicting the proton detected DQ-SQ correlation and the spin state selection. (A) homonuclear active spin states in DQ dimension, (B) spin state selection resulting only from passive spin states $|\alpha\alpha\rangle$, $|\alpha\beta\rangle$, $|\beta\alpha\rangle$ and $|\beta\beta\rangle$ of protons in DQ dimension as ^{19}F is decoupled by refocusing pulse, and (C) Each spin state in B splits in to $|\alpha\rangle$ and $|\beta\rangle$ states of ^{19}F in the SQ dimension.

energy level diagram in Fig. 3. The homonuclear highest quantum achievable in this spin system is 4Q, where all the four protons are allowed to flip simultaneously. This pertains to a spin selective excitation of 4th quantum of a five system. Then all the active protons can be regarded as a super spin with two possible orientations, i.e, $|\alpha\alpha\alpha\alpha\rangle_H$ and $|\beta\beta\beta\beta\rangle_H$ (Fig. 3A). The absence of any pulse on ^{19}F leaves its $|\alpha\rangle$ and $|\beta\rangle$ spin states unperturbed in both F_1 and F_2 dimensions. In such a correlation, 4Q coherence of $|\alpha\rangle$ spin state of ^{19}F is correlated to corresponding $|\alpha\rangle$ spin state of ^{19}F in SQ dimension. The same analogy holds good for $|\beta\rangle$ domain MQ coherence. Thus in 4Q dimension the scalar coupling is absent among the protons and the spins do evolve at the cumulative additive values of their chemical shifts. However, the active spins evolve with the sum of prevailing passive heteronuclear couplings (sum of J_{HF}'s). The two 4Q spin states are further split into a doublet due to $|\alpha\rangle$ and $|\beta\rangle$ spin states of passive ^{19}F (Fig. 3B). From the first order interpretation of the coupling pattern it is obvious that there are sixteen transitions possible for each proton. However, $|\alpha\rangle$ and $|\beta\rangle$ spin states of ^{19}F in 4Q dimension correlate respectively to the corresponding $|\alpha\rangle$ and $|\beta\rangle$ spin states of ^{19}F in the SQ dimension as depicted in Fig. 3C. Thus for each proton eight possible transitions are detected for each $|\alpha\rangle$ and $|\beta\rangle$ spin states of ^{19}F. Therefore, the cross section for particular spin state of ^{19}F results

in half the number of transitions thereby reducing the redundancy in the number of single quantum transitions by a factor of two which is depicted in Fig. 3D.

8. Application of MQ to molecules containing single aromatic ring

In single aromatic ring systems with a substituted NMR active heteronucleus, such as ^{31}P or ^{19}F, the spectral simplification is achieved by the non-selective excitation of homonuclear highest quantum coherence of protons. This is a situation where ^{19}F or ^{31}P acts as a passive spin providing spin state selection. This is demonstrated on the molecules 2-fluoropyridine and 1-chloro-2-fluorobenzene[47]. Both the molecules pertains to weakly coupled spin system of the type AFPKX with ^{19}F as X spin and the remaining spins are protons. The non-selective excitation of 4Q-SQ is achieved by the pulse sequence given in Fig. 1A. The 4Q-SQ spectra along with the chemical structures and numbering of the molecules are reported in Figs. 4B and 4D. Further one can also detect proton 2nd or 3rd quantum coherences in this molecule. The cross section taken along SQ dimension for a particular spin state in the 4Q dimension contains sufficient number of transitions required to determine chemical shifts of all the active spins and all the couplings among them. The relative displacement of cross sections along F_1 dimension

Figure 3: The schematic representation of energy level diagram depicting the 4Q-SQ correlation in AFKPX spin system and the spin state selection achieved in an AFPKX spin system (where X spin is ^{19}F and the remaining spins are protons). (A) homonuclear active spin states in 4Q dimension, (B) spin state selection resulting from the passive spin states $|\alpha\rangle$ and $|\beta\rangle$ of ^{19}F in 4Q dimension and (C) Each $|\alpha\rangle$ and $|\beta\rangle$ spin states of ^{19}F in 4Q correlates to its corresponding $|\alpha\rangle$ and $|\beta\rangle$ states in the SQ dimension giving rise to spin state selection. D) Demonstration of spectral simplification across the passive spin states of ^{19}F.
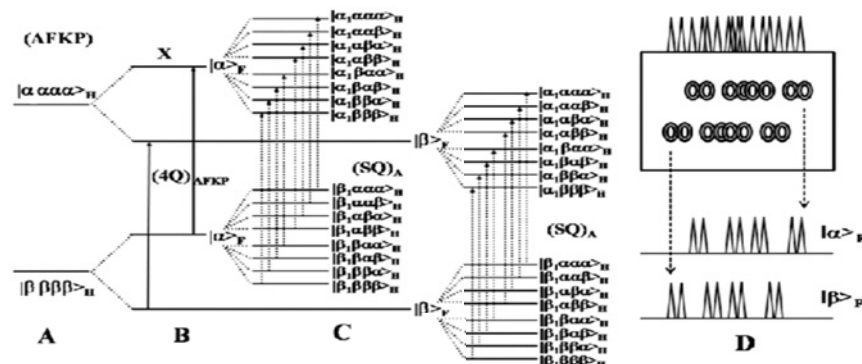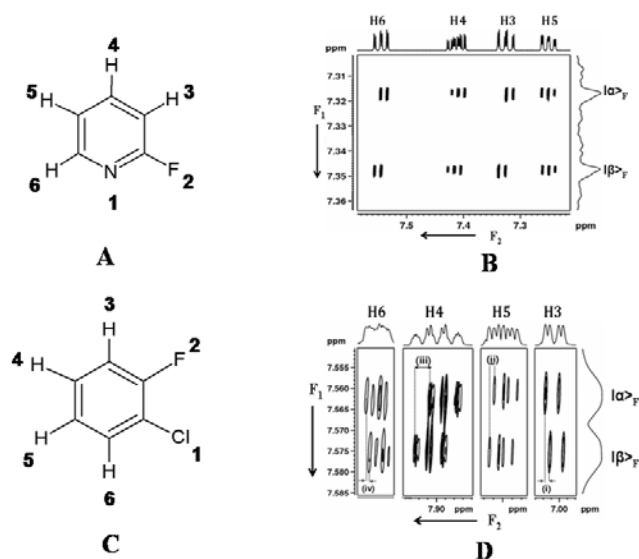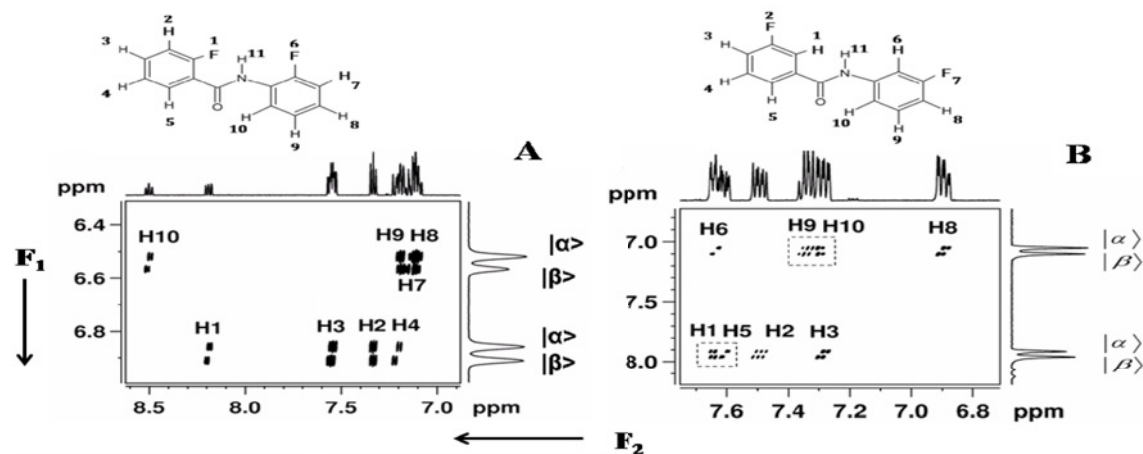
Figure 4: (A) Molecular structure and numbering of interacting spins in 2-Fluoropyridine and (B) 500 MHz ^{1}H 4Q-SQ spectrum of (A). (C) Molecular structure along with numbering of interacting spins 1-chloro-2-fluorobenzene (D) The 500 MHz ^{1}H 4Q-SQ spectrum in the solvent acetone-d$_6$. Two signals along 4Q axis (F$_1$ dimension) corresponded to the $|\alpha\rangle$ and $|\beta\rangle$ spin states of Fluorine separated by the sum of all J$_{HF}$ couplings. The assignment to different protons are also marked for both the molecules. It is evident that the spectral complexity is reduced by a factor of two due to spin-state selection.

at each chemical shift position provides magnitude of heteronuclear couplings. The direction of tilt of the displacement vector provides relative signs of the heteronuclear couplings. Further one can also detect proton 2nd and 3rd quantum coherences in these molecules. These are the situation pertaining to spin state selection of homo/hetero nuclear passive spins in MQ dimension either selectively or non-selectively using pulse sequences given in Fig. 1A or 1B respectively.

Figure 5: (A) The 500 MHz ^{1}H 4Q-SQ correlated spectra of the 2-fluoro-N-(2-fluorophenyl)benzamide along with F_1 and F_2 projections. For A the size of the 2D data matrix is 4096 X 1024. The optimized τ delay is 35.7 ms. The digital resolution in F_1 and F_2 dimensions are 1.66 and 0.23 Hz respectively.; (B) The 500 MHz ^{1}H 4Q-SQ correlation spectrum of 3-fluoro-N-(3-fluorophenyl)benzamide along with F_1 and F_2 projections. The size of the 2D data matrix is 2048 × 1024. The optimized τ delay is 41.67 ms. The time domain data was processed with the sine bell window function in both the dimensions. The digital resolution in F_1 and F_2 dimensions are 1.17 and 0.4 Hz respectively. For both the molecules the time domain data is processed with the sine bell window function in both the dimensions. The four transitions in the 4Q dimension pertain to two spin states of ^{19}F of each phenyl ring marked $|\alpha\rangle$ and $|\beta\rangle$ respectively. Chemical structure and number of interacting protons are given at the top of the 2D Spectra; assignments of chemical shifts for different protons are also marked.

9. Applications of MQ to molecules containing two or more phenyl rings

Although the advantage of MQ excitation is conclusively evident for mono aromatic ring systems, the apparent spectral complexity of multi-aromatic ring systems, such as aromatic polymers, and bio-macromolecules is entirely different. For example aromatic amides are one such interesting family of molecules that find potential applications in building their higher analogues called supramolecular clusters, helical foldamers and dendrimers. The NMR spectral complexity of these molecules drastically increases as the number of phenyl rings in the molecule increases, which in turn is determined by several factors like, isomerism based on the type of hetero atoms as substituents, their chemical and magnetic equivalence[48,49]. Moreover, in the aromatic region the transitions from different phenyl rings overlap in a small spectral width of 1–2 ppm. The spectral complexity also differs significantly depending on the spin topology of the interacting spins in phenyl rings. In the following sections the use of MQ technique for the analyses of spectra for such molecules are discussed.
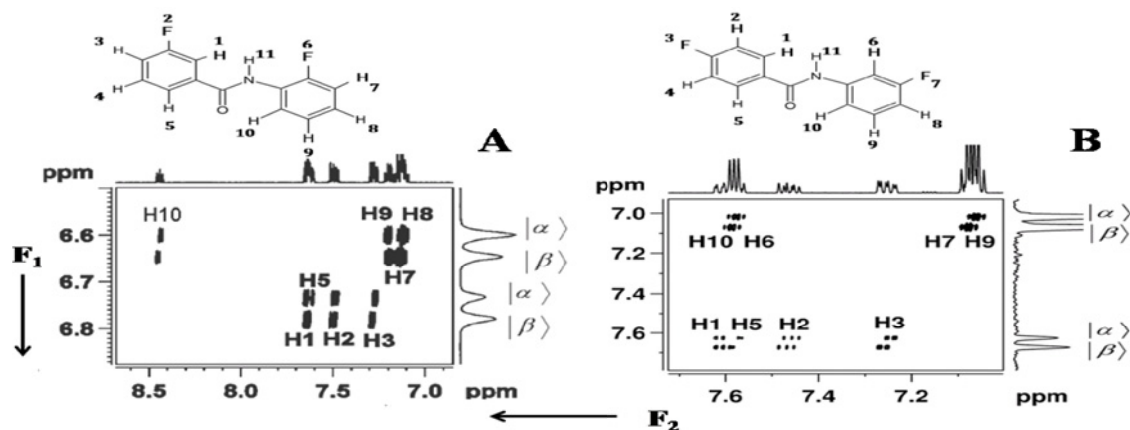
10. Molecules containing two phenyl rings of identical spin topology

The each isomer of benzanilides viz, 2-fluoro-N-(2-fluorophenyl) benzamide and 3-fluoro-N-(3-fluorophenyl)benzamide, contains two phenyl rings

of identical spin topology. The molecular structure along with number of interacting spins is shown in Fig 5. Each molecule has eleven interacting spins. Consequently the complex proton spectrum of the molecule pertains to ten interacting spins with eight protons and two fluorines. It is obvious from the F_2 projections of Fig. 5 that due to degeneracy of the transitions the one dimensional ^{1}H spectrum does not display eight distinct chemical shifts in both the molecules. For the unambiguous analyses of the spectrum, the unravelling of the overlapped transitions is a prerequisite. Being separated by seven bonds, the coupling between interring spins are undetectable and hence the spectrum of each molecule can be construed as an overlap of two independent five spin spectra. In both the molecules, four coupled protons and the fluorine of each phenyl ring pertains to the weakly coupled spin systems of the type AFKPX, where X is the ^{19}F spin and the remaining spins are protons. The ^{1}H detected spectrum is the AFKP part of this AFKPX spin system. The highest homonuclear multiple quantum excitation possible in each of the two independent five spin systems is 4th quantum of protons. The 4Q-SQ correlation spectra of these molecules reported in Fig. 5 clearly identifies the sub-spectra from the two phenyl rings.

In 2-fluoro-N-(2-fluorophenyl)benzamide (Fig. 5A), the difference in the cumulative additive

Figure 6: (A) The 500 MHz ^{1}H 4Q-SQ correlated spectra of the 2-fluoro-N-(3-fluorophenyl)benzamide along with F_1 and F_2 projections. The size of the 2D data matrix is 4096×1024. The optimized τ delay is 166.7 ms. The digital resolution in F_1 and F_2 dimensions are 1.26 and 0.23 Hz respectively; (B) The 500 MHz ^{1}H 4Q-SQ correlation spectrum of 3-fluoro-N-(4-fluorophenyl)benzamide along with F_1 and F_2 projections. The size of the 2D data matrix is 2100×700. The optimized τ delay is 33.33 ms. The data was zero filled to 4096×1024 points before processing. The digital resolution in F_1 and F_2 dimensions are 0.49 and 0.12 Hz respectively. The sine bell window function was used in both the dimensions for processing. In both the molecules, the four transitions in 4Q dimension pertain to two spin states of ^{19}F of each phenyl ring. Chemical structure and number of interacting spins are given at the top of the 2D spectra. The assignment of chemical shift positions for individual protons is marked.
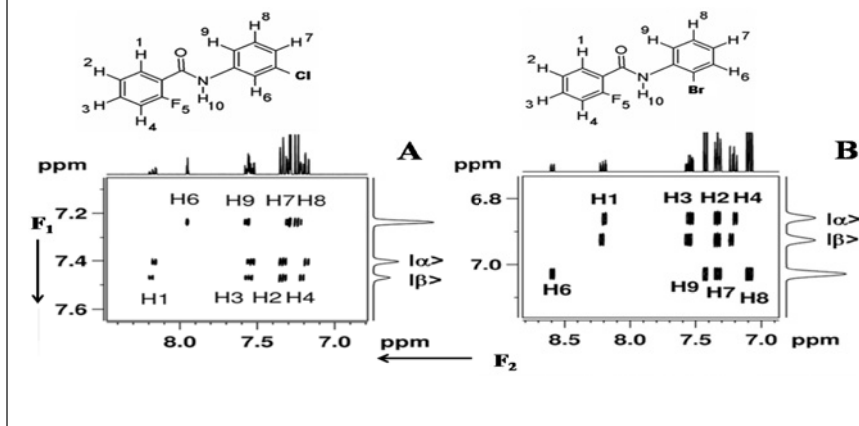

values of all the proton chemical shifts between the phenyl rings $(\delta_{H1} + \delta_{H2} + \delta_{H3} + \delta_{H4}) - (\delta_{H7} + \delta_{H8} + \delta_{H9} + \delta_{H10})$ is 171.54 Hz and the corresponding value in the 4Q dimension is 171.43 Hz. The multiplicity pattern enabled the assignment of the doublet centered at 6.88 ppm in the indirect dimension, to the phenyl ring with spins numbered 1–5. Accordingly the other doublet centered at 6.54 ppm is assigned to the phenyl ring with spins numbered 6-10. The respective doublet separations in the 4Q dimension for these rings are 23.06 and 25.23 Hz. These values are the algebraic sums of all J_{HF} with appropriate sign combination. Similarly, for 3-fluoro-N-(3-fluorophenyl)benzamide , the difference in sum of the chemical shifts $[(\delta_{H6} + \delta_{H9} + \delta_{H10} + \delta_{H8}) - (\delta_{H1} + \delta_{H5} + \delta_{H4} + \delta_{H3})]$ between the phenyl rings is 435.11 Hz and the corresponding value in the 4Q dimension is 435.74 Hz. The doublet centered at 7.94 ppm is assigned to the phenyl ring which has spins numbered 1–5 and the other doublet centered at 7.07 ppm is assigned to the phenyl ring which has spins numbered 6–10. Assignments to individual protons are significantly simplified after separation of the two independent five spin spectra. For both the molecules, cross section taken parallel to F_2 dimension in each phenyl ring position either for $|\alpha\rangle$ or for $|\beta\rangle$ spin state of ^{19}F provides all the proton-proton couplings corresponding to the particular phenyl ring. Thus

the significant simplification achieved by the use of MQ is clearly evident from the sub spectrum of each cross section which contains only one fourth the number of transitions compared to that of the one dimensional ^{1}H spectrum. The assignment of peaks to the individual protons of the phenyl rings is straightforward and is marked in the figure. From the multiplicity pattern many homonuclear couplings could be determined[48,49]. The measure of displacement of the spectra between the cross sections and the inspection of the direction of tilt at the chemical shift position of each proton pertaining to $|\alpha\rangle$ and $|\beta\rangle$ states provided the magnitude of J_{HF} and their relative signs. It is clearly evident that three of the heteronuclear couplings (J_{HF}) have their displacement vectors tilted in the same direction and the tilt of one of the displacement vector is opposite to these three.

11. Molecules containing two phenyl rings with different spin topologies

Unlike the molecules discussed in the previous section, the present section is focussed on the molecules with different spin topologies of the two phenyl rings. The molecular structures and the numbering of atoms along with the 4Q-SQ correlation spectra are given in Fig. 6. In 2-fluoro-N-(3-fluorophenyl)benzamide (Fig. 6A), topology of both the phenyl rings is AFKPX but with different coupled networks of protons. On the other hand

Figure 7: (A) The 400 MHz ^{1}H 4Q-SQ correlated spectra of the 3-chloro-N-(2-fluorophenyl)benzamide along with F_1 and F_2 projections. The size of the 2D data matrix is 2048 × 256. The optimized τ delay is 35.7 ms. The data was zero filled to 4096 × 2048 points before processing. The digital resolution in F_1 and F_2 dimensions are 0.17 and 0.27 Hz respectively; (B) The 400 MHz ^{1}H 4Q-SQ correlation spectrum of 2-bromo-N-(2-fluorophenyl)benzamide along with F_1 and F_2 projections. The size of the 2D data matrix is 2100 × 700. The optimized τ delay is 38.53 ms. The data was zero filled to 4096 × 2048 points before processing. The sine bell window function was used in both the dimensions for processing. The digital resolution in F_1 and F_2 dimensions are 0.15 and 0.39 Hz respectively. In both the molecules, the transitions in the 4Q dimension pertain to two spin states of ^{19}F are marked. The assignment of chemical shift for protons is also given.

in 3-fluoro-N-(4-fluorophenyl)benzamide (Fig. 6B), the spin systems are of the type AA′MM′X and AFKPX. The distinctly different peaks for both the phenyl rings could be filtered out in this molecule also. The first order analyeis of the spectra corresponding to both the phenyl rings in the molecule 2-fluoro-N-(3-fluorophenyl)benzamide and the ring with fluorine in the meta position in the 3-fluoro-N-(4-fluorophenyl)benzamide molecule are carried out analogous to the molecules discussed in the previous section. However, the protons of the phenyl ring with fluorine in the para position form "nearly" an AA′XX′ spin system due to accidental equivalence of some protons and the first order analysis of the spectrum of this strongly coupled spin system is not possible. Furthermore, the cross section taken along SQ dimension at any of the spin state of ^{19}F in the 4Q dimension provided a deceptively simple spectrum with only four transitions of significant intensity. Although heteronuclear couplings with the relative signs are determined precisely for this ring, three of the homonuclear couplings could only be estimated.

12. Dihalogenated benzanilides
In this section we concentrate on the spectra of dihalogen substituted benzanilides. Though the basic molecular framework is similar to difluorinated benzanilides discussed in the previous sections, the substitution of different halogens at

different positions of the phenyl ring drastically alters the complexity of the proton NMR spectra[50]. This is evident from the F_2 projection of the 4Q-SQ for the molecules, 3-chloro-N-(2-fluorophenyl)benzamide and 2-bromo-N-(2-fluorophenyl)benzamide given in Fig. 7. Moreover, the identification of peaks corresponding to fluorinated phenyl ring is another task in these classes of molecules.

MQ analysis of these molecules is similar to those discussed in earlier except the absence of spin-state selection for the phenyl rings substituted with halogens other than fluorine. The 4Q dimension has three peaks, one of which is from the non-fluorinated ring and other is the doublet arising due to heteronuclear splitting with ^{19}F. This enables the easy identification of the peaks for each phenyl ring. The first order analyses of these spectra are pretty straightforward and all the spectral parameters could be measured precisely. Therefore, the higher quantum correlation studies have several distinct advantages in these class of molecules also. They are; (a) filters the sub spectra for different spin systems, (b) reduces the redundancy in the single quantum transitions for each spin state of ^{19}F, (c) simplifies the complexity of the spectrum by a factor of two, as far as the determination of the scalar couplings between the protons of the ^{19}F substituted phenyl ring is concerned, and (d) provides relative signs of the heteronuclear couplings. All these advantages enabled the spectral analyses of all the molecules.

13. Determination of magnitudes of smaller couplings

In all the above examples, the 4Q-SQ correlation experiment fails to resolve very small remote ^{1}H-^{1}H couplings. For example the extraction of remote couplings $^4J_{ij}$ and $^5J_{ij}$ from these experiments are severely hindered as they are of negligible strengths and hidden within the natural line widths. One of the ways of combating this problem is by in the introduction of homonuclear spin state selection of remote passive couplings such as $^5J_{ij}$. For this to be achieved the remote proton must be a passive spin and its spin states should not be disturbed both in MQ and SQ dimensions. Moreover to avoid any further displacement due to spin state selection of ^{19}F spin, the decoupling of ^{19}F spin is essential. The design of such a pulse sequence is possible by selective or biselective excitations of two spins leading to multiple quantum coherence[47]. The pulse sequence for such a technique is reported in Fig. 1C. The application of a non-selective refocusing pulse in such a sequence in the middle of the t_1 dimension on protons mimics ^{19}F decoupling. This is analogous to the spin selective J-resolved experiment employing multiple quantum (MQ) excitations and retains only the active couplings in the double quantum dimension thereby achieving spin state selection. Though small, these remote passive couplings lead to relative displacements which are measurable in such resolved experiments. Depending on the spectral complexity the appropriate 2Q and 3Q-J-resolved technique with a blend of spin state selection have been developed.
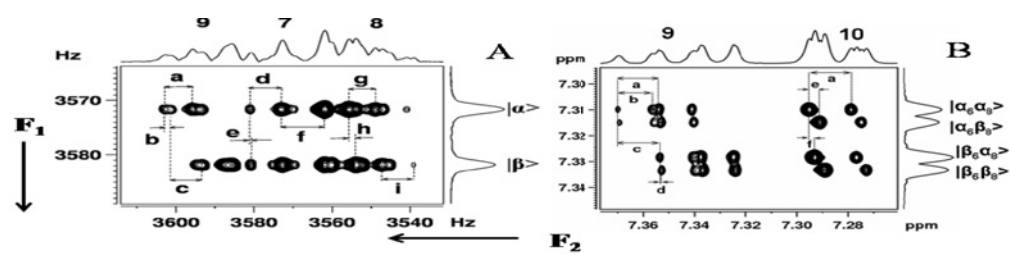
14. Higher quantum J-resolved experiments

In the 4Q-SQ spectrum of the molecule 3-fluoro-N-(3-fluorophenyl)benzamide reported in Fig. 5B, a triplet pattern is observed at the chemical shift position of proton 9. The topology of the spin system suggests that $^3J_{89}$ and $^3J_{9,10}$ are of comparable magnitudes and can account for this triplet. The $^5J_{69}$ coupling is undetectable because of very small magnitude and is hidden in the natural line width. Therefore it is very difficult to determine small remote ^{1}H-^{1}H couplings from the sub spectrum of the 4Q-SQ correlation experiment. This problem has been circumvented by the use of homonuclear spin state selection. For achieving spin state selection the coupling to this remote proton must be retained in both the dimensions and its spin state must not be disturbed during MQ-SQ conversion. It implies that the remote proton must be retained as a passive spin throughout the correlation like a heteronucleus. This necessitates the application of spin selective

pulse and a nonselective refocusing pulse on protons in the middle of MQ dimension to avoid further splitting by ^{19}F spin. However ^{19}F-^{1}H coupling together with active coupling is present in the single quantum dimension. For such an experiment the spin state selective homonuclear MQ-J-resolved pulse sequence has been developed and is reported in Fig. 1C. In order to measure all the remote couplings, two independent spin selective DQ-J resolved (SSDQ-J-resolved) experiments have been performed on this molecule. The Fig. 8B contains the spin selective DQ-J-resolved spectrum with selective excitation of protons 9 and 10 and with the simultaneous application of a nonselective 180° pulse on protons in the middle of t_1 dimension. In the DQ dimension the pulse sequence retains only the sum of passive couplings to protons 6 and 8 (i.e. $J_{69} + J_{6,10}$ and $J_{89} + J_{8,10}$) while the couplings to fluorine spin are completely refocused. In such a situation the remaining two passive protons (6 and 8) of the phenyl ring mimics the heteronuclei. Each of the protons 6 and 8 has spin states $|\alpha\rangle$ and $|\beta\rangle$ and in the spin product basis has four Eigen states $|\alpha_6\alpha_8\rangle$, $|\alpha_6\beta_8\rangle$, $|\beta_6\alpha_8\rangle$ and $|\beta_6\beta_8\rangle$, where the subscript refers to protons 6 and 8. The spin states of the passive protons are not disturbed providing spin state selection. Thus the DQ dimension will have four transitions with the large doublet separation providing $J_{89} + J_{8,10}$, while the smaller doublet separation provides $J_{69} + J_{6,10}$. The separation in the DQ dimension would be identical at the chemical shift positions of both the active spins. In the SQ dimension there are two displacement vectors for each of the spins 9 and 10 which provide both active and passive couplings. The two displacements at the chemical shift position of proton 9 can be utilized to determine individual values of J_{89} and J_{69}. The displacements at the chemical shift position of proton 10 can be exploited to derive individual values of $J_{8,10}$ and $J_{6,10}$. Thus from this experiment the couplings, which were difficult to extract from the 4Q-SQ experiment, could be determined more precisely. The technique also overcomes the problem of field inhomogeneity contributions because of the application of 180° pulse in the middle of the t_1 dimension.

As far as the extraction of the coupling among protons in the phenyl ring with protons numbered 7–10 is concerned, it is very tedious due to severe overlap of the transitions from the protons 7, 8 and 9. This is due to identical spin topology in all the molecules. Therefore, the selective excitation of any two protons of this ring is impossible without disturbing the remaining protons. However, selective excitation of protons 7, 8 and 9 is not precluded. Therefore analogous to SSDQ-J-resolved

Figure 8: (A) The SS3Q-J-resolved spectrum of 2-fluoro-N-(2-fluorophenyl)benzamide in the isotropic solvent $CDCl_3$ with the selective excitation of protons 7, 8 and 9. The size of the 2D data matrix is 4096×2048. The number of t_1 increments is 128. The time domain data was processed with the sine bell window function in both the dimensions. The digital resolution in F_1 and F_2 dimension are 0.02 and 0.01 Hz respectively. The seduced shape pulses are of duration 8.33 m is used for the selective excitation with optimized τ delay is of 62.5 m. The marked spin states $|\alpha\rangle$ and $|\beta\rangle$ in the 3Q dimension corresponds to the passive spin states of proton 10. Displacements provide the coupling information are a = J_{89}, b = J_{79}, c = J_{910}, d = J_{78}, e = $J_{7,10}$, f = J_{67}, g = J_{78}, h = $J_{8,10}$ and i = J_{89}. Notice the smaller values of the coupling, $J_{7,10}$ that could be measured from this experiment which was difficult to obtain from the other experiments. The direction of the tilts indicate that the couplings $J_{7,10}$, $J_{8,10}$ and $J_{9,10}$ have similar signs. B) The SSDQ-J-resolved spectra of 3-fluoro-N-(3-fluorophenyl)benzamide in the isotropic solvent $CDCl_3$; Spectrum corresponding to the selective double quantum excitation of protons 9 and 10. The size of the 2D data matrix is 512×96. The optimized τ delay is 2.08 ms. The data was zero filled to 2048×1024 points before processing. The sine bell window function was used in both the dimensions for processing. The digital resolution in F_1 and F_2 dimension are 0.07 and 0.06 Hz respectively. The displacements providing the coupling information are; a = $J_{9,10}$, b = J_{79}, c = J_{89}, d = J_{69}, e = $J_{8,10}$ and f = $J_{6,10}$. The marked spin states in the DQ dimension corresponds to the passive spins 6 and 8.

experiment, the novel SS3Q-J-resolved experiment has been carried out[50]. The decoupling of ^{19}F by the π pulse in the t_1 dimension, provides a doublet in the 3Q dimension due to splitting from the $|\alpha\rangle$ and $|\beta\rangle$ spin states of passive proton 10 with a separation equal to the sum of all the couplings to the passive spin $(J_{7,10} + J_{8,10} + J_{9,10})$. The displacement of cross sections aided the direct measure of $^3J_{HH}$, $^4J_{HH}$ and $^5J_{HH}$ to proton 10. The displacements and the resonance separations providing the couplings are marked in Fig. 8A. The inspection of the directions of the tilts marked in the figure reveals that $^3J_{HH}$, $^4J_{HH}$ and $^5J_{HH}$ have similar signs. The combined analyses of 4Q-SQ correlated, SSDQ-J-resolved and SS3Q-J-resolved experiments provided the precise values of long range couplings in all the molecules.

15. Advantages of averaged τ optimization in SSMQ-J-resolved experiments
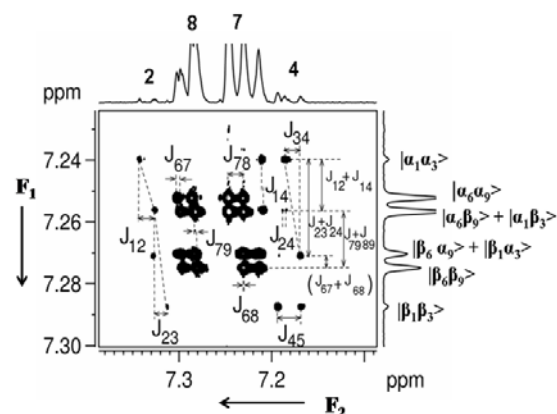
In a complex situation, in one of the molecules displayed in Fig. 7 (3-chloro-N-(2-fluorophenyl)benzamide), it is impossible for the selective excitation of any two protons without disturbing the spins from the other ring as the transitions are severely overlapped. Thus, the derivation of remote couplings employing DQ-J-resolved experiment in such situations is challenging. In combating this difficulty the knowledge of approximate coupling strengths has been used for

optimizing of the τ delay for selective excitation of protons in the crowded region. The bunch of resonances (H7 and H8) is dominated by scalar coupling J_{78} (nearly 8 Hz) rather than J_{24} (nearly 2 Hz). The averaged τ delay has been appropriately optimized for the DQ excitation of protons H2, H4, H7 and H8. There is an excellent suppression of the transitions corresponds to the protons H2 and H4 as the strength of coherence transfer is insufficient to enhance the signal intensity. Moreover, the signals along DQ axis are distinctly separated to provide the required coupling information. This is obvious from the two-dimensional (2D) spectrum reported in Fig. 9. Analysis of this spectrum has thus been significantly simplified. Precise long-range couplings that were difficult to extract from the one-dimensional spectrum could be determined.

16. Numerical analyses of the spectra

In order to determine the accuracy of precision of experimental parameters, the numerical iterative analysis has also been carried out on selected molecules discussed in the previous sections. The conventional numerical iterative analyses of one dimensional spectra are tedious for all the molecules due to severe degeneracy of the transitions. However, the analysis of any one of the cross sections corresponding to $|\alpha\rangle$ and $|\beta\rangle$ spin states of ^{19}F provides homonuclear couplings and the combined analysis of transitions corresponding to both the

Figure 9: (A) The spectrum corresponding τ-averaged spin selective DQ J resolved for the protons H2, H4, H7 and H8 for the molecule shown in Fig 7A. The marked spin states in the DQ dimension corresponds to the passive spins 1, 3, 6 and 9. The displacements providing the coupling information are J_{12}, J_{14}, J_{23}, J_{24}, J_{34}, J_{45}, J_{67}, J_{68}, J_{78}, J_{79} and J_{89}. Notice the distinct advantage of the experiment in measuring the precise values of the smaller couplings (J_{14} and J_{68}) which were otherwise difficult to measure.

section of the single quantum dimension at the spin state of the passive spin in the MQ dimension. The displacement of the cross sections and the direction of the tilt of the displacement vectors at the chemical shift positions of each proton provided the magnitudes and relative signs of the couplings. The novel spin selective double and triple quantum J-resolved experiments aided the determination of remote couplings of smaller magnitudes which are hidden within the line widths. The systematic studies on several isomers of halogen substituted benzanilides reveal that the $^5J_{HF}$ is negative in all the molecules irrespective of their spin topologies.

18. Acknowledgements

References
1. T. J. Norwood, Prog. NMR Spectrosocpy, **24**, 295 (1992).
2. G. Bodenhausen, Prog. NMR Spectrosocpy, **14**, 137 (1980).
3. NMR Spectroscopy, Basic Principles, Concepts, and Applications in Chemistry, H. Günther, John Wiley and Sons, New York, 1992.
4. Principles of Nuclear Magnetic Resonance in One and Two dimensions, R. R. Ernst, G. Bodenhausen and A. Wokaun, Clarendon Press, Oxford, 1991.
5. Understanding NMR Spectroscopy, J. Keeler, John Wiley and Sons, England, 2005.
6. D. Neuhaus, G. Wagner, M. Vasak, J. H. R, Kaegi and K. Wuthrich, Eur. J. Biochem. **151**, 257 (1985).
7. L. E. Kay and A. Bax, J. Magn. Reson. **86**, 110 (1990).
8. S. Heikkinen, H. Aitio, P. Permi, R. Folmer, K. Lappalaonen and I Kilpelainen, J. Magn. Reson. **137**, 243 (1999).
9. A. Bax and R. Freeman, J. Magn. Reson. **44**, 542 (1981).
10. C. Griesinger, O. W. Sorensen and R. R. Ernst, J. Chem. Phys. **85**, 6837 (1986).
11. P. Pfandler and G. Bodenhausen, J. Magn. Reson. **72**, 475 (1987).
12. G. T. Montelione, M. E. Winker, P. Rauenbuehler and G. Wagner, J. Magn. Reson. **82**, 198 (1989).
13. O. W. Sørensen, J. Magn. Reson., **90**, 433 (1990).
14. C. Griesinger, O. W. Sørensen and R. R. Ernst, J. Am. Chem. Soc. **107**, 6394 (1985).
15. U. Eggenberger, Y. Karimi-Nejad, H. Thüring, H. Rüterjans and C. Griesinger, J. Biomol. NMR, **2**, 583 (1992).
16. J. M. Schmidt, R. R. Ernst, S. Aimoto and M. Kainosho, J. Biomol. NMR, **6**, 95 (1995).
17. A. Bax, D. Max and D. Zax, J. Am. Chem. Soc., **114**, 6923 (1992).
18. B. Reif, M. Köck, R.Kerssebaum, J.Schleucher and C. Griesinger, J. Magn. Reson. B, **112**, 295 (1996).
19. J. S. Hu and A. Bax, J. Am. Chem. Soc. **119**, 6360 (1997).
20. H. Oschkinat, A. Pastor, P. Pfändler, G. Bodenhausen, J. Magn. Reson. **69**, 559 (1986).
21. R. Brüschweiler, J. C. Madsen, C. Griesinger, O. W. Sørensen and R. R. Ernst, J. Magn. Reson. **73**, 380 (1987).
22. R. Freeman, Mol. Phys. **4**, 385 (1961).
23. W. S. Brey, L. W. Jaques and H. J. Jakobsen, Org. Magn. Reson., **12**, 243 (1979).
24. J. Jarvet and P. Allard, J. Magn. Reson. B **112**, 240 (1996).
25. P. Permi, S. Heikkinen, I. Kilpeläinen and A. Annila, J. Magn. Reson., **139**, 273 (1999).

spin states provides both homo and heteronuclear couplings pertaining to each phenyl ring. The chemical shifts and the couplings determined by the higher quantum correlation and resolved experiments were used as the starting parameters and were further refined using numerical iteration. The experimentally measured values of couplings were in close agreement with the numerically calculated ones.

17. Conclusions

The one dimensional proton spectra of molecules containing many aromatic rings are very complex with severe overlap of transitions. The analyses of such spectra demand the discerning of degenerate transitions. In this review a brief discussion is provided on the recently reported multiple quantum techniques in combating such difficulties. The developed methodologies employ selective and non-selective excitation and detection of higher quantum correlations. Irrespective of the spin topologies of the different phenyl rings, the non-selective excitation of homonuclear highest quantum coherence results in filtering of sub spectra for each aromatic ring, provided there is substantial difference in the cumulative additive values of proton chemical shifts of each spin system in the higher quantum dimension. This spin system filtering combined with spin state selective detection reduces the redundancy in the detected single quantum transitions. This significantly simplifies the analyses of the ^{1}H spectra taken along the cross

26. G. Otting, J. Magn. Reson., **124**, 503 (1997).

27. A. Rexroth, P. Schmidt, S. Szalma, T. Geppert, H. Schwalbe, and C. Griesinger, J. Am. Chem. Soc., **117**, 10389 (1995).

28. P. Anderson, J. Weigelt and G. Otting, J. Biomol. NMR, **12**, 435 (1988).

29. B. Brutscher, J. Magn. Reson. **151**, 332 (2001).

30. P. Permi, J. Magn. Reson. **163**, 114 (2003).

31. L . Duma, S. Hediger, A. Lesage and L. Emsley, J. Magn. Reson. **164**, 187 (2003).

32. L. Duma, S. Hediger, B. Brutscher, A. Böckmann and L. Emsley, J. Am. Chem. Soc., **125**, 11816 (2003).

33. P. Nolis, J. F. Espinosa and T. Parella, J. Magn. Reson. **180**, 39 (2006).

34. R. Verel, T. Manolikas, A.B. Siemer, B.H. Meier, J. Magn. Reson. **184**, 322 (2007).

35. P. Permi and A. Annila, J. Biomol. NMR, **20**, 127 (2001).

36. P. Permi and A. Annila, J. Biomol. NMR. **16**, 221 (2000).

37. P. Permi, J. Biomol. NMR. **22**, 27 (2002).

38. D. Lee, B. Vögeli and K. Pervushin, J. Biomol. NMR, **31**, 273 (2005).

39. P. Würtz, K. Fredriksson and P. Permi, J. Biomol. NMR, **31**, 321 (2005).

40. Christy Rani R. Grace and R. Riek, J. Am. Chem. Soc., **125**, 16104 (2003)

41. P. Nolis and T. Parella, J. Biomol. NMR, **37**, 65 (2007).

42. P. R. Vasos, J. B. Hall and D. Fushmann, J. Biomol. NMR, **31**, 149 (2005).

43. L. Braunschweiler, G. Bodenhausen ; R.R. Ernst, Molecular Physics, **1983**, 48 (3), 535–560.

44. N. Murali, Y. V. S. Ramakrishna, K. Chandrasekhar, M. Albert Thomas and Anil Kumar, Pramana, **23**, 547 (1984).

45. M. H. Levitt and R. R. Ernst, *Chem. Phys. Lett.* **1983**, 100, 119.

46. M. H. Levitt and R. R. Ernst, *J. Chem. Phys.* **1985**, 83, 3297.

47. Bikash Baishya and N. Suryaprakash, J. Chem. Phys. **127**, 214510 (2007).

48. G. N. Manjunatha Reddy, T. N. Guru Row and N. Suryaprakash, J. Magn. Reson. **196**, 119–126 (2009).

49. B. Bikash, G.N. Manjunatha Reddy, R. P. Uday, T. N. Guru Row and N. Suryaprakash, J. Phys. Chem. A **112**, 10526–10532 (2008).

50. G. N. Manjunatha Reddy, Susanta Kumar Nayak, T. N. Guru Row and N. Suryaprakash, Magn. Reson. Chem. **47**, 684–692 (2009).

G.N. Manjunatha Reddy received his masters in chemistry in 2007 from Bangalore University, Bangalore, India. Soon after he pursued his research career at NMR Research Centre, Indian Institute of Science, Bangalore, India, working on Multiple Quantum NMR methods for the spectral simplification of scalar and dipolar coupled spins. Currently he holds an undergraduate studentship at Institute des Sciences Moléculares de Marseille, Marseille, France.

N. Suryaprakash, Ph.D. 1986, Bangalore University, Bangalore (supervisors Prof. C.L. Khetrapal and Prof. G.K. Narayana Reddy), Postdoctoral research at University of Basel, Switzerland, 1990–91 (Prof. Peter Diehl), Ben Gurion University of the Negev, Israel; 1998–1999 (Prof. Raz Jelinek) University of Southampton, United Kingdom 1999–2000 (Prof. J.W. Emsley). Presently Faculty of NMR Research Centre, Indian Institute of Science, Bangalore. Fellow of National Academy of Sciences, Allahabad, India. Research Interests: Development of multi dimensional single quantum and multiple quantum NMR Methodologies. Structures of molecules in the liquid crystalline media, NMR Methods for the study of enantiomers, weak molecular interactions.